Galaxy Evolution and Feedback across Different Environments
Proceedings IAU Symposium No. 359, 2020
T. Storchi-Bergmann, W. Forman, R. Overzier & R. Riffel, eds.
doi:10.1017/S1743921320004032

ORAL CONTRIBUTIONS

Tracing young SMBHs in the dusty distant universe – a Chandra view of DOGs

Karín Menéndez-Delmestre[1], Laurie Riguccini[1] and Ezequiel Treister[2]

[1]Valongo Observatory, Federal University of Rio de Janeiro,
Ladeira Pedro Antônio 43, Centro, Rio de Janeiro, RJ, Brazil
email: kmd@astro.ufrj.br

[2]Pontificia Universidad Católica, Instituto de Astrofísica,
Vicuña Mackenna 4860, Macul, Santiago, Chile

Abstract. The coexistence of star formation and AGN activity has geared much attention to dusty galaxies at high redshifts, in the interest of understanding the origin of the Magorrian relation observed locally, where the mass of the stellar bulk in a galaxy appears to be tied to the mass of the underlying supermassive black hole. We exploit the combined use of far-infrared (IR) Herschel data and deep Chandra ∼160 ksec depth X-ray imaging of the COSMOS field to probe for AGN signatures in a large sample of >100 Dust-Obscured Galaxies (DOGs). Only a handful (∼20%) present individual X-ray detections pointing to the presence of significant AGN activity, while X-ray stacking analysis on the X-ray undetected DOGs points to a mix between AGN activity and star formation. Together, they are typically found on the main sequence of star-forming galaxies or below it, suggesting that they are either still undergoing significant build up of the stellar bulk or have started quenching. We find only ∼30% (6) Compton-thick AGN candidates ($N_H > 10^{24}$ cm^{-2}), which is the same frequency found within other soft- and hard-X-ray selected AGN populations. This suggests that the large column densities responsible for the obscuration in Compton-thick AGNs must be nuclear and have little to do with the dust obscuration of the host galaxy. We find that DOGs identified to have an AGN share similar near-IR and mid-to-far-IR colors, independently of whether they are individually detected or not in the X-ray. The main difference between the X-ray detected and the X-ray undetected populations appears to be in their redshift distributions, with the X-ray undetected ones being typically found at larger distances. This strongly underlines the critical need for multiwavelength studies in order to obtain a more complete census of the obscured AGN population out to higher redshifts. For more details, we refer the reader to Riguccini *et al.* (2019).

Keywords. galaxies: active, galaxies: evolution, galaxies: high-redshift

1. Introduction

Massive galaxies continue to pose important challenges to our current understanding of galaxy formation. Stellar population studies and the presence of an underlying supermassive black hole (SMBH) point to the idea that these galaxies are the result of mergers between gas-rich galaxies. Within this formation scenario, a dust-obscured phase – where starburst episodes coexist with activity from a galactic nucleus (AGN) associated to the growth of a young SMBH – is traced back to the so-called ultra-luminous infrared (IR) galaxies (ULIRGs: $L_{IR} > 10^{12} L_{\odot}$; Sanders *et al.* 1988). ULIRGs are locally rare, but appear to dominate the co-moving energy density at higher redshifts ($z > 2$; e.g., Casey *et al.* 2014). Many of these galaxies have been identified by the detection of their thermal dust emission at submillimeter wavelengths (the so-called submillimeter galaxies or SMGs; Blain *et al.* 1999). Detailed ground-based follow-up in the optical/near-IR and mm/radio, as well as space-based studies with Chandra, HST and Spitzer have revealed intricate morphologies reminiscent of major mergers (e.g., Swinbank *et al.* 2010; Engel *et al.* 2010; Alaghband-Zadeh *et al.* 2012; Menéndez-Delmestre *et al.* 2013), and the predominance of (weak) AGN, establishing that star formation and AGN activity coexist in these objects (e.g., Chapman *et al.* 2005; Alexander *et al.* 2005; Pope *et al.* 2008; Menéndez-Delmestre *et al.* 2009). Other dusty galaxies have been selected by their high dust obscuration in optical bands (F24/FR>1000) and named 'dust-obscured galaxies' or DOGs (Dey *et al.* 2008). They are typically characterized by a rising power-law continuum of hot dust (∼200–1000 K) in the near-IR, indicating that their mid-IR luminosity is dominated by an AGN and that they likely trace a later phase in the merger-ULIRG scenario (e.g., Riguccini *et al.* 2015).

Riguccini *et al.* (2015) showed that a sub-sample of DOGs with far-IR (100–500μm) detection have a significant contribution from AGN activity at higher IR luminosities. Although X-ray surveys are a powerful tool to select unobscured and mildly-obscured AGNs, the current census of actively-growing SMBHs still remains far from complete (e.g, Treister *et al.* 2004; Worsley *et al.* 2005; Tozzi *et al.* 2006; Page *et al.* 2006; Fiore *et al.* 2009; Juneau *et al.* 2013). Because DOGs are selected based on their far-IR output, at longer wavelengths than the AGNs selected by near-through-mid IR surveys, far-IR selected DOGs can potentially represent a distinctly-defined population of AGN candidates. In this work we exploit the Chandra COSMOS Legacy Survey (Civano *et al.* 2016) to assess the AGN fraction in DOGs using the most recent and exquisite combination of far-IR and X-ray data. We here focus in the main results and refer the reader to Riguccini *et al.* (2019) for further details and discussion.

2. Far-IR DOGs and the search for X-ray counterparts in the Chandra COSMOS Legacy Survey

We build our "far-IR DOG" parent sample using the catalogues provided by the PEP and HerMES Herschel surveys (Berta *et al.* 2011; Roseboom *et al.* 2010) to identify DOGs in the COSMOS field, all detected in at least 3 of the 5 Herschel bands. We identified a total of 108 far-IR DOGs, 22 with spectroscopic redshifts from Salvato *et al.* (in prep.) and the rest with photometric redshifts determined by Riguccini *et al.* (2015).

The Chandra COSMOS Legacy Survey (Civano *et al.* 2016) covers a total area of $\sim$2.2 deg^2, uniformly covering the $\sim$1.7 deg^2 COSMOS/HST field at a $\sim$160 ksec depth, expanding on the deep C-COSMOS area (1.45 vs 0.44 deg^2) by a factor of $\sim$3 at $\sim 3 \times 10^{16}$ erg cm^{-2} s^{-1}. The deeper and wider coverage of the Chandra COSMOS Legacy survey compared to previous X-ray observations of the COSMOS field (e.g., Brusa *et al.* 2007, 2010; Salvato *et al.* 2009) allows us to detect new X-ray DOGs that have been missed by previous X-ray surveys. We identify individual X-ray counterparts for 22 of the far-IR DOGs. From these 22, 9 are detected in X-rays for the first time thanks to the increased field coverage of the Chandra COSMOS Legacy Survey.

Stacking of the DOGs with no individual X-ray detections suggests a mixture of star-formation and AGN activity. Stacking also showed that X-ray fluxes increase with 24 μm flux (see also Dey *et al.* 2008 and Fiore *et al.* 2009), pointing to an increase of the total AGN fraction in the brightest 24 μm bins. This indicates that the combined population of X-ray detected and far-IR DOGs is effective at selecting AGNs, compared to the 24 μm population as a whole.

3. Obscured hosts and the search for Compton-thick AGNs

Because of low number counts, detailed fitting to the observed X-ray spectrum is not possible for the majority of the X-ray detected DOGs. However, we were able to estimate the neutral hydrogen column density along the line of sight (N_H) based on the methodology described in Treister *et al.* (2009) which assumes an intrinsic power-law spectrum with spectral index $\Gamma = 1.9$ (corresponding to the observed average AGN spectrum; Nandra & Pounds 1994) and computes the expected hardness ratio (HR) for the source (more details in Riguccini *et al.* 2019). Using this approach we find that 6 out of the 22 X-ray detected DOGs (i.e., 27%) are plausible Compton-thick AGNs ($N_H > 10^{24}\mathrm{cm}^{-2}$), 15 are moderately-obscured AGNs (10^{22} cm$^{-2} < N_H < 10^{24}$ cm^{-2}), and only one has a low hardness-ratio consistent with being unobscured ($N_H < 10^{22}\mathrm{cm}^{-2}$).

The fraction of Compton-thick AGNs that we find in our sample is consistent with previous local and low-redshift reports (e.g., Georgakakis *et al.* 2010; Ricci *et al.* 2015; Aird *et al.* 2015; Burlon *et al.* 2011). In particular, based on NuSTAR observations at 5-80 keV – with a sensitivity peak at 10-30 keV – the observed fraction is 11-20% (Civano *et al.* 2015; Masini *et al.* 2018), while Lansbury *et al.* (2017) report a fraction of ∼30% based on the NuSTAR Serendipitous survey. It would have been reasonable to expect DOGs to have a higher fraction of Compton-thick sources because by definition they have dustier host galaxies. However, our results appear to indicate that there is no significant difference with the general AGN population. Thus, we can speculate that the obscuration, at least in the most extreme cases has to be nuclear and roughly independent of the properties of the host galaxy (see also Ricci *et al.* 2015; Buchner & Bauer 2017).

4. DOGs with AGN signatures – a step closer to quenching

In Figure 1 (left panel) we show the evolution of the specific star-formation rate (sSFR = SFR/M*) of DOGs with cosmic time. The SFR rate is calculated from the IR luminosity obtained from the SED-fitting analysis of Riguccini *et al.* (2015), after the AGN contribution has been removed. The stellar masses are from Ilbert *et al.* (2009), based on the SED fits of 30 bands from the COSMOS survey. We immediately note that DOGs with no AGN signatures based on the far-IR lie on the Main Sequence of star-forming galaxies and within the starburst regime (Riguccini *et al.* 2015). The stacking of all X-ray undetected DOGs also places this population within the main-sequence region. On the other hand, the DOGs with AGN signatures (both in the X-ray and the far-IR) predominantly appear to present lower sSFRs, occupying the region of the main-sequence or below it. Considering that these dust-enshrouded galaxies, where both star formation and AGN coexist, likely trace stages in the merger-ULIRG-quasar scenario called upon to explain the formation of massive galaxies (e.g., Hopkins *et al.* 2008; Toft *et al.* 2014), Figure 1 suggests that DOGs with an AGN signature may be a subpopulation that is further ahead in the ULIRG-quasar scenario, already quenching the star-formation activity.

Only two DOG sources with AGN signatures lie well above the main sequence: one Compton-thick candidate and a moderately obscured AGN. According to the evolutionary scenario of Treister *et al.* (2010), the highly obscured Compton-thick phase corresponds to the early, very dust-enshrouded phase of a major merger where a SMBH is rapidly growing, while the moderately obscured AGN phase traces a later stage in this evolutionary scenario, when feedback from the AGN has already started heating up the dust and gas of the galaxy, shutting down star formation activity. In this picture, we would expect Compton-thick candidates to lie slightly above the moderately-obscured AGNs in the sSFR-redshift diagram. We do not observe this in Figure 1. This further

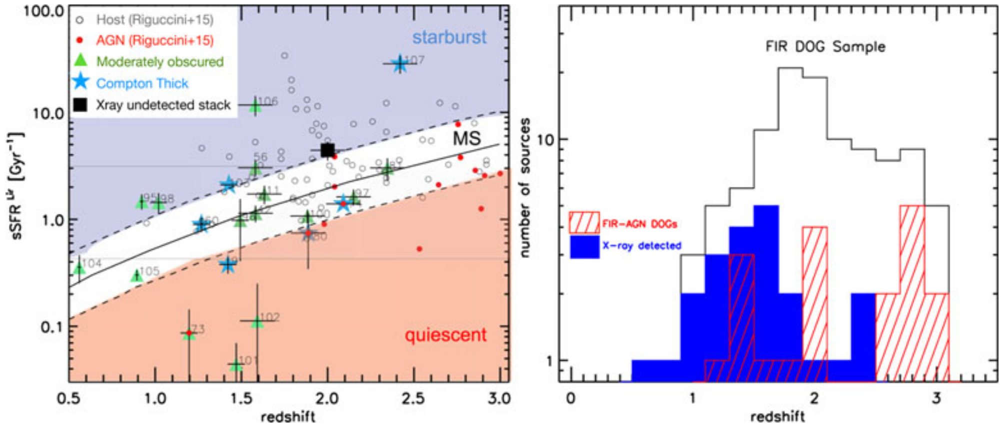

Figure 1. [Left Panel]: Evolution of the specific SFR (sSFR) of DOGs with cosmic time. DOGs with no AGN signatures (empty circles, identified as "host") based on the far-IR analysis of Riguccini *et al.* (2015) lie on the Main Sequence of star-forming galaxies and within the starburst regime. DOGs identified to have an AGN either based on the far-IR (red circles) or X-ray (green triangles and blue stars; this work) predominantly lie on the Main Sequence or below. This suggests that this AGN sub-population of DOGs may already be quenching star formation and be in a latter phase of the ULIRG-quasar scenario. [Right Panel]: Redshift distribution of the DOG parent sample (black histogram), which includes 108 DOGs detected in at least 3 of the five Herschel bands (100–500 μm). The filled and hatched histograms highlight DOGs with AGN signatures in the X-ray (based on the present work) and mid-to-far-IR SED fitting analysis from Riguccini *et al.* (2015), respectively. The two populations only seem to differ in their redshift distributions. This emphasizes the need for a multi-band approach to get a full census of the obscured AGN population out to higher redshifts. Figure from Riguccini *et al.* (2019).

supports that, at least for the most extreme sources, the obscuration is nuclear and thus not directly connected to the evolutionary stage of the host galaxy.

We also bring to the attention of the reader that both DOGs with AGN signatures detected in the X-ray and those detected in the far-IR share the same behaviour vis-a-vis their position with respect to the main sequence of star-forming galaxies: they are typically found on the main-sequence or below it. They also typically display similar near-IR and mid-to-far IR colors. The main difference between these populations appears to be in their redshift distribution (Figure 1, right panel). The DOGs with AGN signatures in the far-IR are typically found at higher redshifts than those with X-ray signatures. Together, these results suggest that the two populations share most of their physical properties and that the lack of detection in the X-ray band for the bulk of far-IR AGN DOGs is explained by the difference in redshift distributions. This emphasizes the crucial need for a multi-wavelength approach to obtain a more complete census of the obscured AGN population out to higher redshifts.

We report here the X-ray and far-IR properties of 108 DOGs from the COSMOS field. Considering that selection criteria of the DOG sample (i.e., F24/FR>1000) selects $z \sim 2$ highly dust-enshrouded galaxies in the LIRG/ULIRG regime, there was an expectation to uncover privileged sites of highly-obscured AGNs with a higher frequency of Compton-thick AGNs. However, ~70% are moderately obscured AGNs ($N_H \sim 10^{22-24}$ cm^{-2}) and only ~30% (6) Compton-thick AGN candidates ($N_H > 10^{24}$ cm^{-2}). This is the same as within other AGN populations, so the fact that by looking at DOGs we are indeed going after more heavily-obscured AGNs seems to make no difference. That is, the large N_H of Compton-thick AGNs must be nuclear and have little to do with the dust obscuration from the host galaxy. However, with a higher fraction of AGNs (based on X-ray and far-IR analysis) than the whole 24μm population, DOGs present an interesting population

https://doi.org/10.1017/S1743921320004032 Published online by Cambridge University Press

to select AGN candidates at higher redshifts (moderately, highly-obscured). This work emphasizes the important role that the DOG population, in particular the combined X-ray and far-IR detected DOG population, plays in the effort to get a more complete census of the AGN population at high redshift, particularly for the highly obscured population.

References

Alaghband-Zadeh, S., Chapman, S. C., Swinbank, A. M., *et al.* 2012, *MNRAS*, 424, 2232
Alexander, D. M., Bauer, F. E., Chapman, S. C., *et al.* 2005, *ApJ*, 632, 736
Aird, J., Coil, A. L., Georgakakis, A., *et al.* 2015, *MNRAS*, 451, 1892
Berta, S., Magnelli, B., Nordon, R., *et al.* 2011, *A&A*, 532, A49
Blain, A. W., Small, I., Ivison, R. J., *et al.* 1999, "The Hy-Redshift Universe: Galaxy Formation and Evolution at High Redshift", ASP Conference Proceedings, vol. 193, eds. A. J. Bunker and W. J. M. van Breugel, p. 425
Brusa, M., Zamorani, G., Comastri, A., *et al.* 2007, *ApJ Supplement Series*, 172, 353
Brusa, M., Civano, F., Comastri, A., *et al.* 2010, *ApJ*, 716, 348
Buchner, J. & Bauer, F. E. 2017, *MNRAS*, 465, 4348
Burlon, D., Ajello, M., Greiner, J., *et al.* 2011, *ApJ*, 728, 58
Casey, C. M., Narayanan, D., & Cooray, A. 2014, *Physics Reports*, 541, 45
Chapman, S. C., Blain, A. W., Smail, I., *et al.* 2005, *ApJ*, 622, 772
Civano, F., Hickox, R. C., Puccetti, S., *et al.* 2015, *ApJ*, 808, 185
Civano, F., Marchesi, S., Comastri, A., *et al.* 2016, *ApJ*, 819, 62
Dey, A., Soifer, B. T., Desai, V., *et al.* 2008, *ApJ*, 677, 943
Engel, H., Tacconi, L. J., Davies, R. I., *et al.* 2010, *ApJ*, 724, 233
Fiore, F., Puccetti, S., Brusa, M., *et al.* 2009, *ApJ*, 693, 447
Georgakakis, A., Rowan-Robinson, M., Nandra, K., *et al.* 2010, *MNRAS*, 406, 420
Hopkins, P. F., Hernquist, L., Cox, T. J., *et al.* 2008, *ApJ Supplement Series*, 175, 356
Ilbert, O., Capak, P., Salvato, M., *et al.* 2009, *ApJ*, 690, 1236
Juneau, S., Dickinson, M., Bournaud, F., *et al.* 2013, *ApJ*, 764, 176
Lansbury, G. B., Alexander, D. M., Aird, J., *et al.* 2017, *ApJ*, 846, 20
Masini, A., Civano, F., Comastri, A., *et al.* 2018, *ApJ Supplement Series*, 235, 17
Menéndez-Delmestre, K., Blain, A. W., Smail, I., *et al.* 2009, *ApJ*, 699, 667
Menéndez-Delmestre, K., Blain, A. W., Swinbank, M., *et al.* 2013, *ApJ*, 767, 151
Nandra, K. & Pounds, K. A. 1994, *MNRAS*, 268, 405
Page, M. J., Loaring, N. S., Dwelly, T., *et al.* 2006, *MNRAS*, 369, 156
Pope, A., Bussmann, R. S., Dey, A., *et al.* 2008, *ApJ*, 689, 127
Ricci, C., Ueda, Y., Koss, M. J., *et al.* 2015, *ApJ Letters*, 815, L13
Ricci, C., Bauer, F. E., Treister, E., *et al.* 2017, *MNRAS*, 468, 1273
Riguccini, L., Le Floc'h, E., Mullaney, J. R., *et al.* 2015, *MNRAS*, 452, 470
Riguccini, L. A., Treister, E., Menéndez-Delmestre, K., *et al.* 2019, *AJ*, 157, 233
Roseboom, I. G., Oliver, S. J., Kunz, M., *et al.* 2010, *MNRAS*, 409, 48
Salvato, M., Hasinger, G., Ilbert, O., *et al.* 2009, *ApJ*, 690, 1250
Sanders, D. B., Soifer, B. T., Elias, J. H., *et al.* 1988, *ApJ*, 325, 74
Swinbank, A. M., Smail, I., Chapman, S. C., *et al.* 2010, *MNRAS*, 405, 234
Toft, S., Smolčić, V., Magnelli, B., *et al.* 2014, *ApJ*, 782, 68
Tozzi, P., Gilli, R., Mainieri, V., *et al.* 2006, *A&A*, 451, 457
Treister, E., Urry, C. M., Chatzichristou, E., *et al.* 2004, *ApJ*, 616, 123
Treister, E., Cardamone, C. N., Schawinski, K., *et al.* 2009, *ApJ*, 706, 535
Treister, E., Urry, C. M., Schawinski, K., *et al.* 2010, *ApJ Letters*, 722, L238
Worsley, M. A., Fabian, A. C., Bauer, F. E., *et al.* 2005, *MNRAS*, 357, 1281